

# Fluid–Structure Interaction Analysis in an Atherosclerosis Carotid Artery



Gineesh M. Pillai, J. S. Jayakumar, and R. Ajith Kumar

## *Nomenclature*

$C$	Damping factor (Kns/m)
$d$	Incompressibility (dimensionless)
$f$	External body force (N/m <sup>3</sup> )
$\bar{I}_1$	First-order strain rate (dimensionless)
$\bar{I}_2$	Second-order strain rate (dimensionless)
$J$	Elastic deformation gradient (Pa)
$K$	Structural stiffness (N/m)
$m$	Structural mass (Kg)
$P$	Force vector (N)
$\dot{U}$	Velocity vector (m/s)
$U$	Displacement vector (m)
$v$	Velocity vector (m/s)
$W$	Strain energy potential (J)

## *Greek Symbols*

$\eta$	Viscosity of blood (Ns/m <sup>2</sup> )
$\rho$	Density of blood (Kg/m <sup>3</sup> )
$\sigma$	Stress tensor (N/m <sup>2</sup> )

---

G. M. Pillai · J. S. Jayakumar (✉) · R. A. Kumar  
Department of Mechanical Engineering, Amrita Vishwa Vidyapeetham, Amritapuri, India

## 1 Introduction

Atherosclerosis, or atherosclerotic cardio vascular disease, is a life-threatening condition that can start its early development during childhood. It is a process by which minute deposits of fatty materials known as “plaque” build up inside the walls of the arteries and reduces or completely blocks the oxygen-rich blood flow overtime. In extreme conditions, such cases can lead to a life-threatening heart attack or a sudden stroke. Atherosclerosis comes with a variety of risk factors that include high blood pressure, obesity, high cholesterol, smoking, physical inactivity, and diabetes. The hemodynamics in carotid artery results in limited blood supply to the area surrounding the partially blocked artery, which can end up degrading and potentially killing the neighboring tissues. Significant damage to brain tissues can result in ischemia, along with high wall shear stress and high blood pressure. In atherosclerotic plaque carotid, artery causes the plaque rupture and it leads to complete block in blood vessel.

There are many studies reported on carotid artery disease in the literature. Some of the studies are based on the experimental methods, and others are based on numerical investigations. In the experimental studies reported in the past, the focus was to examine the effects of mechanical forces using particle image velocimetry (PIV) method. Perktold et al. [1] conducted the numerical study of pulsatile, non-Newtonian blood flow in three dimensions on common carotid artery (CCA) under different bifurcation angles using finite element analysis (FEA). This study focuses on the flow and stress properties of different sinus angle variations. They concluded that the stress is affected on the sinus, due to the complex flow at the reattachment zone, flow separation and high wall shear stress on the blood vessels. All of these are important in atherogenesis. Perktold with Rappitsch [2] investigated numerical simulations of local blood flow and vessel mechanics in a carotid artery bifurcation to determine the mechanical stresses in the CCA wall. Urquiza et al. [3] investigated CCA blood flow using multidimensional modeling. This work involves a comparison of the compliant 1D and 3D models of CCA bifurcation using finite element method. They concluded that the blood flow patterns contribute to the development of vascular disease. Zhao et al. [4] conducted a numerical study based on both blood effects and vessel effects employing a realistic physiological model of human CCA bifurcation. Their model was generated from an MRI data and in order to get the results, they implemented combined commercial code of CFX4 and ABAQUS. They revealed that the wall shear stress reduces with respect to pulsatile blood flow and wall movement. A CFD study carried out by Gharahi et al. [5] compares various viscosity models for hemodynamic study on different geometries of human carotid artery that extracted from MRI data (patient-specific study). Sousa et al. [6] conducted fluid–structure interaction (FSI) study of bloodstream in a non-stenosed basic carotid artery bifurcation. This investigation was completed by utilizing vascular geometries that made from Doppler ultrasound pictures. In this study, they explored the impact of hemodynamics of blood, pressure dissemination on the bifurcation region, and lowermost extreme wall shear stress (WSS) at the bifurcation region.

From the literature survey, it is found that the following aspects of atherosclerosis CCA were not studied, viz. plaque rupture in the common carotid artery, hyper-elasticity nature of blood vessel, three layers of the carotid artery wall, and the nature of plaque. Figure 1c shows a typical picture of atherosclerosis CCA (complex atheroma). These aspects being important from medical point of view are taken up in the present study for a numerical investigation. This current study is on the CCA, which is situated in the neck region of the human body (Fig. 1a). CCA supplies blood, oxygen, and nutrients for the brain. A blockage in a CCA artery can cause brain ischemia, brain hypoxia, or brain infarction/ ischemic stroke. This study also aims to provide a dynamic model for the common carotid artery to analyze the flow effects and predict the plaque initiation. This model could predict the chance of initiation of another plaque formation inside the blood vessel.

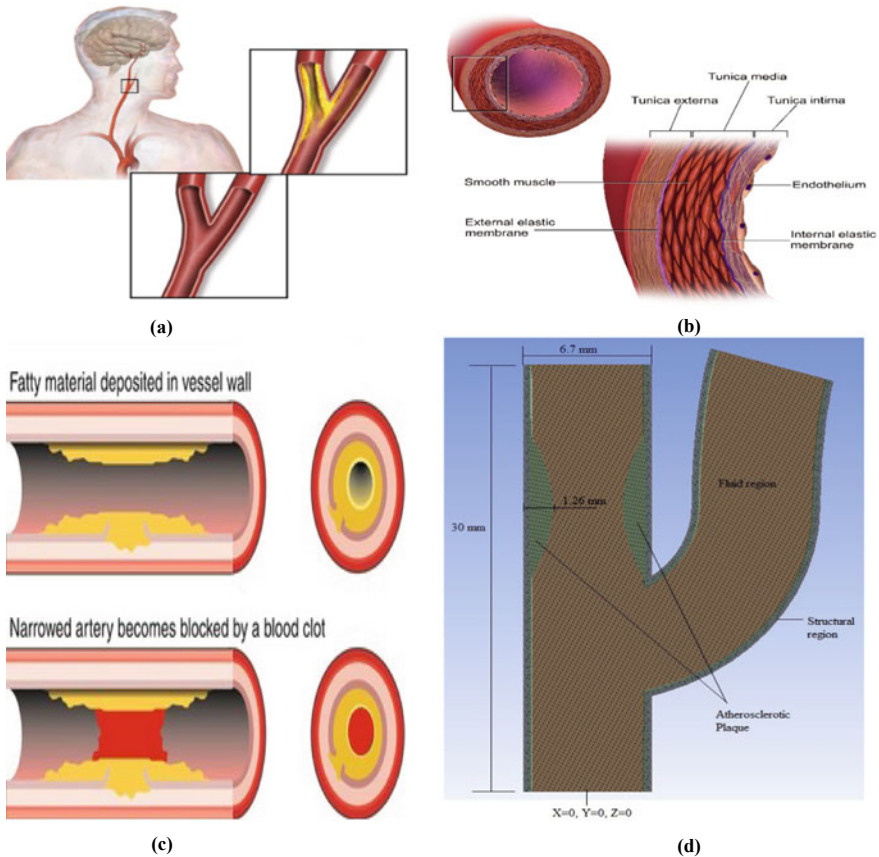


**Fig. 1** a Atherosclerosis in the carotid artery [15]. b Three layers of artery wall. c Atherosclerotic CCA cross section. d Artery narrowed by plaque [15]

## 2 Methodology

### 2.1 Geometry

The artery is modeled as 3D, three layered, (tunica intima or intima, tunica media or media, and tunica externa or adventitia) shown in Fig. 1b, and the plaque is modeled as three-dimensional circular shape, the inner diameter of the stenosis region is 5.72 mm, and the length of the plaque is 5 mm (plaque shoulder). The maximum height of the plaque is 1.26 mm and normal diameter of blood vessel is 6.7 mm; each layer has different hyperelastic property and thickness such as: 0.23, 0.31, and 0.34 mm [7] for intima, media, and adventitia, respectively. The total length of the model is 30 mm, shown in Fig. 1d. Figure 1d shows that the cross-sectional view of atherosclerosis carotid artery bifurcation modeled by ANSYS V19.1. In this geometry, the artery has three layers with atherosclerotic plaque. The plaque has been situated in the intima layer, which has to be considered as the same property of intima layer.

### 2.2 Solid Structure Characteristics

In transient structural analysis, the impulsive load from a source undergoes a structural response which was determined from fluid analysis. In this analysis, the magnitude of forces, deformations, stress, and strain were calculated at small intervals of time. The basic governing equation for structural analysis adopted from coupled fluid–structure interaction [8] is as follows:

$$m\ddot{U} + C\dot{U} + KU = P(t). \quad (1)$$

In this analysis, the structural damping factor is not considered, so that the equation changes to

$$m\ddot{U} + kU = P(t) \quad (2)$$

This modeling of three-layer material was adopted from Holzapfel et al. [9]. The properties displayed by the plaque are taken as same as the intima layer. The hyperelasticity property of each layer is taken from Gholipour et al. [7] The materials were modeled using the formulation given by the Mooney-Rivlin 5 parameter. The parameter equation is as follows;

$$W = -C_{01}(3 - \bar{I}_2) - C_{10}(3 - \bar{I}_1) + C_{11}(3 - \bar{I}_1)(3 - \bar{I}_2) + \frac{1}{d}(1 - J)^2 + C_{20}(3 - \bar{I}_1)^2 + C_{02}(3 - \bar{I}_2)^2 \quad (3)$$

**Table 1** Mooney–Rivlin 5-parameter model material constants [8]

Material	$C_{10}$	$C_{01}$	$C_{20}$	$C_{11}$	$C_{02}$
Intima	$-2.04E + 05$	$2.03E + 05$	$1.37E + 06$	$-3.71E + 06$	$2.67E + 06$
Media	$-1.17E + 05$	$1.28E + 05$	$2.24E + 05$	$-6.72E + 05$	$5.69E + 05$
Adventitia	$-1.89E + 05$	$2.02E + 05$	$4.59E + 05$	$-1.38E + 06$	$1.34E + 06$

In this equation, there are five material constants. These were derived from the curve fitting data as shown in Table 1. The density of each layer is considered as  $1000 \text{ kg/m}^3$  Chan et al. [10].

### 2.3 Fluid Characteristics

Fluid flow domain was mathematically modeled by the Navier–stokes equations. The conservation of mass, momentum, for an incompressible fluid in 3D, can be expressed as:

$$\nabla \cdot v = 0 \quad (4)$$

$$\frac{\rho \partial u}{\partial t} + \rho v \nabla v = \nabla \cdot \sigma + f \quad (5)$$

The external body force is considered as zero. The stress tensor can be expressed as:

$$\sigma = -PI + \tau \quad (6)$$

The blood has been modeled as transient pulsatile motion, with a non-Newtonian behavior. In order to modeling of its non-Newtonian nature, power law is enabled, which is taken from Mandal et al. [11].

$$\eta = \eta_0 \gamma^{n-1} \quad (7)$$

where,  $\eta_0 = 0.035$ ,  $n = 0.6$ ,  $T = 310\text{K}$  Density of blood is taken as  $\rho_{\text{Blood}} = 1060 \text{ kg/m}^3$ ,  $\eta$  denotes viscosity of blood from cilia et al. [12]. The blood flow is treated as transient pulsatile flow profile exceeds up to 0 to 0.8 s, i.e., for one heartbeat. The inlet flow velocity range of common carotid artery is  $0.5$  to  $0.8 \pm 0.3 \text{ m/s}$ , and the inlet velocity profile has shown in Fig. 4 Perktold et al. [1].

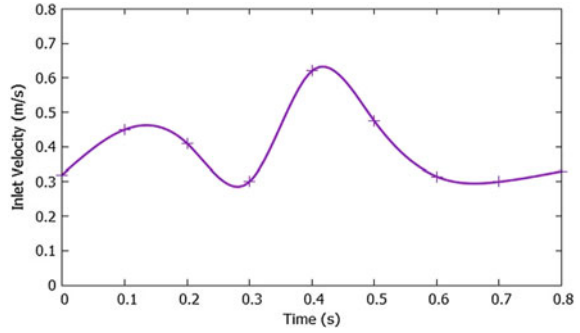
### 3 Solution Method

The important portion of this study is fluid–structure interaction. The common carotid artery is modeled within the ANSYS using the two-way FSI system coupling method. The general condition is transient. Structural analysis is done by transient structural analysis, and fluid analysis is done in the Fluent analysis. These systems are coupled with “system coupling.” The data is transferred from fluid to structural and structural to fluid. The boundary is not rigid, therefore “Dynamic mesh” method was used for this simulation. In dynamic mesh parameter, it should be “smoothing and remeshing,” for dynamic mesh parameter, diffusion method was used, and the value was taken as 0.45. Because if diffusion parameter is zero, mesh will equally be displaced across the domain. The maximum value of diffusion parameter is 2. When maximum displacement will be felt in the far field boundary, a value between 0.4 and 0.45 is good enough. For remeshing, the local cell and local face providing mesh scale parameters from mesh scale info were used. First mesh would distort itself and try to smooth the mesh first as possible as it could. However, once the quality of mesh on the faces across the limit of 0.7 or in case of volume reached is beyond the 0.9, remeshing will be done. The smoothing algorithm will work and beyond these limits of the mesh quality, remeshing will take place. The solution methods used as follows: For the spatial discretization, coupled scheme is used, and least square cell-based gradients are used for this solution. Pressure is discretized in second-order upwind scheme, and for transient formulation, first-order implicit method is used. The mesh is tetrahedral type elements and time step is set to 0.001 s. Fluid solid interface is set to system coupling region, the blood is enter from the bottommost portion of artery. The coupling system transfers converged values of the fluid model solver to the structural model solver. The interpolation of pressure (obtained from fluid solver) is the input data of structural model solver. The converged value of structural analysis is transfer to the fluid model solver. The interpolation of displacement (obtained from transient structural analysis) will be the input data of fluid model solver. This process will continue till the end of the time step.

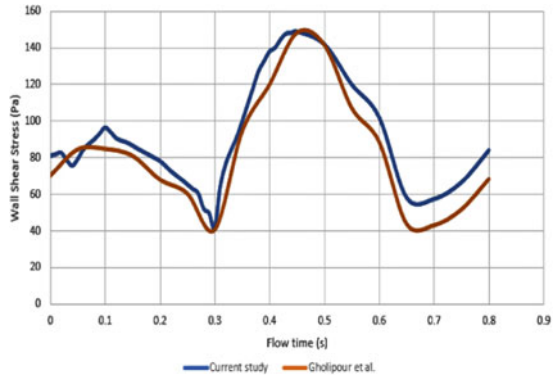
#### 3.1 Numerical Validation

Gholipour et al. [7] had developed a simple model of coronary artery. Their study has demonstrated the effects of three layers of artery and its hyperelasticity where blood displayed a non-Newtonian behavior. They discovered that the maximum wall shear stress acts at the tip of the plaque and its value is 145 Pa. We recreated the same model and corresponding factors to get the results for the present study. The wall shear stress distribution with respect to time for Gholipour et al. and present work is plotted in Fig. 2b. Figure 2b shows that current result (wall shear stress distribution) is in good agreement with that of Gholipour et al. and hence, our numerical model is validated. For CCA geometry, the mesh element size is the same in both fluid

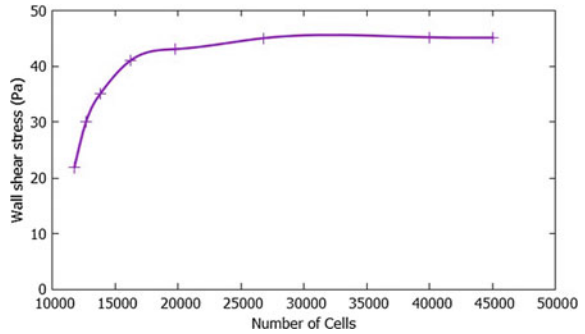
**Fig. 2** **a** Inlet velocity profile perktold et al. [7]. **b** Numerical validation of WSS with Gholipour et al. [8]. **c** Grid independency study



(a)



(b)



(c)

and structural analysis with the tetrahedral mesh-type method. The systematic grid independency study is done by changing the grid count. Figure 2c shows that for a representative accuracy of WSS is attained with the cell numbers 28915. This study reveals that the precision will not be increased even if the cell number increased beyond the above-mentioned cell number.

### 4 Results and Discussions

From this analysis, the results obtained are the blood vessel deformation due to physiological blood pulsation and the dynamic characteristics of blood such as blood pressure, wall shear stress, and its velocity with varying time for one pulsating period. The maximum velocity at the inlet of CCA is 0.65 m/s as shown in Fig. 2a. From the velocity vector contour (Fig. 3a), it could be seen that the velocity is reduced to 0.45 m/s in the bifurcation region  $x = 0$  mm,  $y = 15$  mm,  $z = 0$  mm. Velocity attains the maximum value at the most vulnerable region (stenosis region). The maximum velocity at the stenosis region is 0.79 m/s at  $x = 0$ ,  $y = 20$  mm,  $z = 0$  as shown in Fig. 3b (velocity along the vertical direction of left carotid artery). The main source of structural wall deformation is blood pressure. Figure 3c shows the variation of blood pressure, wall shear stress and von Mises stress in the CCA bifurcation region during one pulsatile period. It could be seen that, all these parameters attain their respective

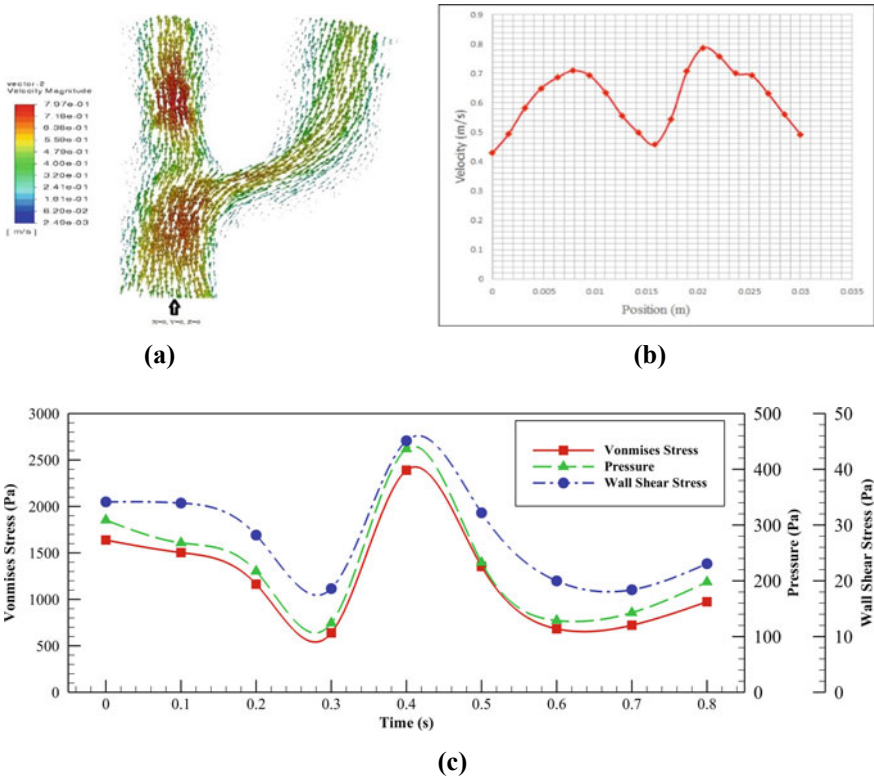


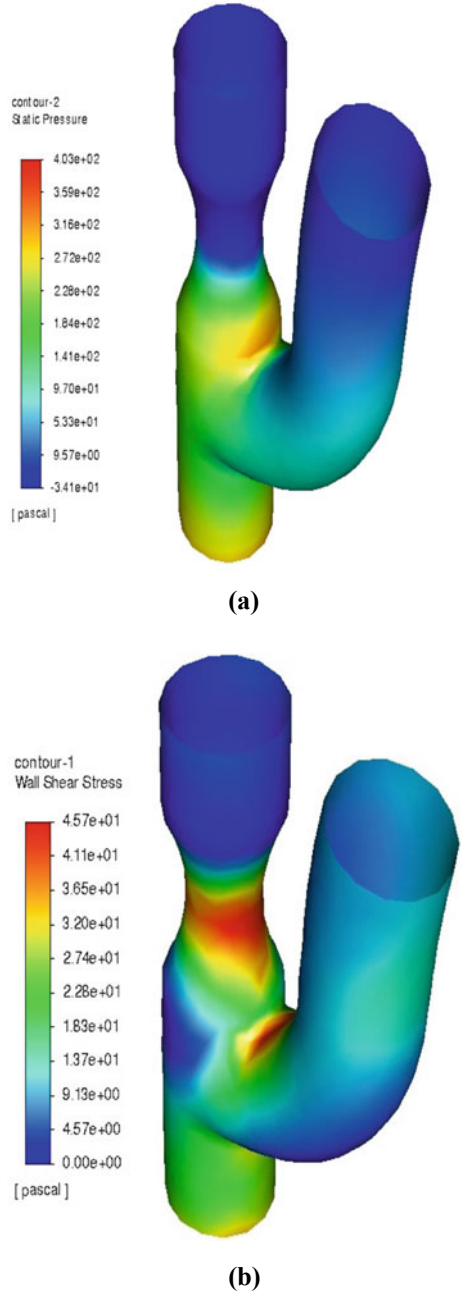
**Fig. 3** a Velocity vector contour ( $t = 0.4$  s). b Velocity position (vertical graph  $x = 0$ ,  $y = 15$  mm,  $z = 0$ ) c Numerical results of wall shear stress ( $t = 0.4$  s,  $x = 20$  mm,  $y = 20$  mm and  $z = 0$ ), effective von Mises stress ( $t = 0.4$  s,  $x = 2.715$  mm,  $y = 15$  mm,  $z = 0$ ), pressure ( $t = 0.4$  s,  $x = 2.715$ ,  $y = 17$  mm,  $z = 0$ ) with respect to time

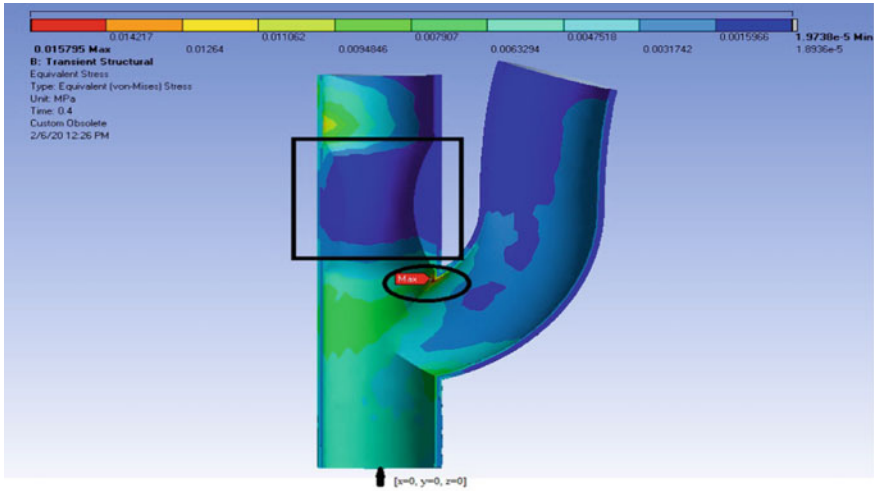


maximum values at  $t = 0.4$  s. The presence of plaque reduces the blood pressure. The pressure contour illustrates that the minimum pressure region is at the maximum stenosis region or the middle portion of atherosclerotic plaque. The minimum blood pressure (9.57 pa) is obtained at  $x = 2.175$  mm,  $y = 20$  mm,  $z = 0$  from Fig. 4a. The location of maximum pressure (403 Pa) is between the bifurcation wall and the point of initiation of stenosis region ( $x = 2.175$  mm,  $y = 15$  mm,  $z = 0$  at  $t = 0.4$  s) as marked in Fig. 4a. As mentioned before, temporal variation of wall shear stress is shown in Fig. 4b with the maximum of 45 Pa at  $t = 0.4$  s, and  $x = 1.675$  mm,  $y = 20$  mm,  $z = 0$ . The highest wall shear stress occurs at the neck region (stenosis region) or the tip of the plaque which could cause the fibrous cap to rupture. The von Mises stress is used to predict yielding of materials under complex loading [13]. In this study, the source of the load is high blood pressure. The pulsating blood flow exerts some forces on the blood vessels layer by layer. Due to this, the blood vessel undergoes a vascular dilation and subsequent contraction because of its hyperelastic nature. There are three layers such as intima, media, and adventitia wherein each one has different elastic properties. In these layers, adventitia is more rigid than the other two. Media layer more flexible than other two layers and the innermost layer is intima. The atherosclerotic plaque is situated in the intima layer. Von Mises stress contour in the intima layer is shown in Fig. 5a. The von Mises stress contour represents the maximum stress values at the maximum elongation and maximum contraction stages of blood vessel. Variation of average value of von Mises stress (effective equivalent stress) with respect to time is shown in Fig. 3c which shows that the maximum averaged value is 2480 pascals at  $t = 0.4$  s and  $x = 2.715$  mm,  $y = 17$  mm,  $z = 0$ . From these results, it could be inferred that the blood flow is greatly affected by the presence of atherosclerotic plaque. Because of the plaque, the value of von Mises stress is minimum in posterior regions (media, adventitia). In general, the vascular dilation and contraction of blood vessel regulate the blood flow. It could be seen that the von Mises stress value attains a minimum for all the layers as shown in Fig. 5b, c in their respective plaque regions. The self-contraction of the media layer is responsible for the blood flow from CCA to capillaries. The presence of atherosclerosis causes a deficiency in active contraction or elongation of blood vessel layers.

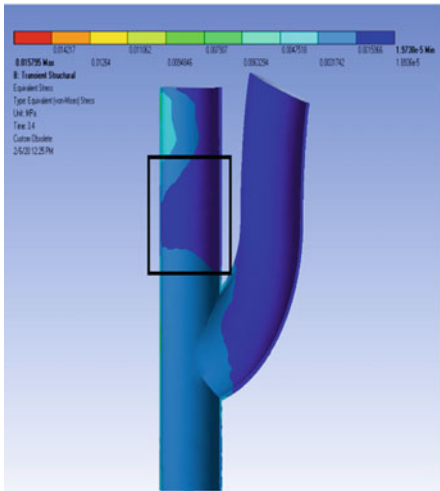
Due to this problem, the blood does not reach the cells and organs in the human body and causes ischemic stroke. Falk shaw et al. [14] conducted an experimental study which reveals that plaque rupture condition range is about 45–50% of vessel stenosis level. In the current study, 45% of stenosis level condition of blood vessel is considered which denotes a possible rupture condition of plaque. Therefore, the present results are expected to provide valuable insight in to the diagnostics of atherosclerosis, by analyzing various stenosis conditions, which helps to diagnosis in atherogenesis.

**Fig. 4 a** Pressure distribution (contour) in of CCA bifurcation at  $t = 0.4$  s.  
**b** Wall shear stress distribution (contour) in CCA bifurcation at  $t = 0.4$  s

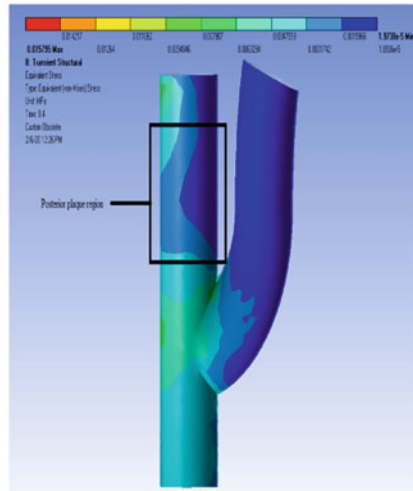




(a)



(b)



(c)

Fig. 5 **a** Von Mises stress in intima layer at  $t = 0.4$  s, **b** von Mises stress in media layer  $t = 0.4$  s, and **c** von Mises stress at adventitia at  $t = 0.4$  s

## 5 Conclusion

This work succeeded to develop a numerical model of an atherosclerotic carotid artery. The model developed is expected to help in the examination of the effect of different factors on a diseased carotid artery. More specifically, the model for the artery and plaque could help to predict the initiation of stroke, or brain ischemia

accurately. The blood pulsation, non-Newtonian flow of blood, and three layers of an artery are essential for predicting the consequences of atherosclerosis artery. These parameters that exert their influences on the atherosclerotic carotid artery can be considered as a realistic representation of plaque behavior. Results indicate that stenosis condition of blood flow causes a reduction in blood pressure by 54%. In the stenosis region, von Mises stress is minimum. Results further indicate that the maximum wall shear stress acts on the fibrous cap (plaque tip).

## References

1. Perktold, K., Resch, M., & Florian, H. (1991). Pulsatile non-Newtonian flow characteristics in a three-dimensional human carotid bifurcation model. *ASME Journal of Biomechanical Engineering*, *113*, 464–475.
2. Perktold, K., & Rappitsch, G. (1995). Computer simulation of local blood flow and vessel mechanics in a compliant carotid artery bifurcation model. *Journal of Biomechanics*, *28*, 845–856.
3. Urquiza, S. A., Blanco, P. J., & Venere, M. J. (2005). Multidimensional modelling for the carotid artery blood flow. *Computer Methods in Applied Mechanics and Engineering*, *195*(2006), 4002–4017.
4. Zhao, S. Z., Xu, X. Y., Hughes, A. D., & Thom, S. A. (2000). Blood flow and vessel mechanics in a physiologically realistic model of a human carotid arterial bifurcation. *Journal of Biomechanics*, *33*(2000), 975–984.
5. Gharahi, H., Zambrano, B. A., Zhu, D. C., DeMarco, J. K., & Baek, S. (2016). Computational fluid dynamic simulation of human carotid artery bifurcation based on anatomy and volumetric blood flow rate measured with magnetic resonance imaging. *Int J Adv Eng Sci Appl Math*, *8*(1), 46–60. <https://doi.org/10.1007/s12572-016-0161-6>.
6. Sousa, L. C., Castro, C. F., António, C. C., & Azevedo, E. (2009). Fluid-structure interaction modeling of blood flow in a non-stenosed common carotid artery bifurcation. In *Proceedings of the 7th International Conference on Mechanics and Materials in Design*. Albufeira/Portugal 11–15 June 2017. Editors J.F. Silva Gomes and S.A. Meguid. Publ. INEGI/FEUP (2017)
7. Gholipour, M. H., Ghayesh, A. Z., & Mahajan, R. (2018). Three-Dimensional Biomechanics of coronary artery. *International Journal of Engineering Science*, *130*, 93–114.
8. Raja, R. S. (2012). Coupled fluid structure interaction analysis on a cylinder exposed to ocean wave loading. CHALMERS, *Applied Mechanics*, Master's Thesis 2012, 55
9. Holzapfel, G. A., Sommer, G., Gasser, C. T., & Regitnig, P. (2005). Determination of layer-specific mechanical properties of human coronary arteries with nonatherosclerotic intimal thickening and related constitutive modeling. *American Journal of Physiology-Heart and Circulatory Physiology*, *289*, H2048–H2058.
10. Chan, W., Ding, Y., & Tu, J. (2007). Modeling of non-Newtonian blood flow through a stenosed artery incorporating fluid-structure interaction. *Anziam Journal*, *47*, 507–523.
11. Mandal, M. S., Mukhopadhyay, S., & Layek, G. (2012). Pulsatile flow of an incompressible, inhomogeneous fluid in a smoothly expanded vascular tube. *International Journal of Engineering Science*, *57*, 1–10.
12. Cilla, M., Borrás, I., Pena, E., Martínez, M., & Malve, M. (2015). A parametric model for analysing atherosclerotic arteries: On the FSI coupling. *International Communications in Heat and Mass Transfer*, *67*, 29–38.
13. Lian, H., Christiansen, A. N., Tortorelli, D. A., Sigmund, O., & Aage, N. (2017). Combined shape and topology optimization for minimization of maximal von Mises stress. *Structural and Multidisciplinary Optimization*, *55*, 1541–1557. <https://doi.org/10.1007/s00158-017-1656-x>
14. Falk, E., Shah, P. K., & Fuster, V. (1995). Coronary plaque disruption. *Circulation*, *92*, 657–671.

***Online document***

15. <https://www.cookmedical.com/peripheral-intervention/health-and-wellness-ways-to-prevent-or-ease-the-symptoms-of-pad/>